Research Article

Coupling between Human Brain Cortical Thickness and Glucose Metabolism from Regional to Connective level: a PET/MRI study

Qi Huang[1], Yihong Yang[2], Na Qi[2], Yihui Guan[1], Jun Zhao[2], Fengchun Hua[3], Shuhua Ren[1], Fang Xie[4]

1. Department of Nuclear Medicine & PET Center, Huashan Hospital, Shanghai, China; 2. Department of Nuclear Medicine, Tongji University School of Medicine, Shanghai, China; 3. Department of Nuclear Medicine, Longhua Hospital Shanghai University of Traditional Chinese Medicine, Shanghai, China; 4. Huashan Hospital, Shanghai, China

Objectives: Disruption of the balance between brain structure and function is implicated in many brain disorders. This study aimed to investigate the coupling between the brain cortical thickness (CTh) and glucose metabolism using ^{18}F-FDG PET/MRI.

Methods: 138 subjects who performed brain ^{18}F-FDG PET/MRI were retrospectively recruited and divided into two groups according to their ages. The Spearman's rank correlation was calculated between the FDG uptakes and CTh across the cortex for each subject to explore the structural and functional coupling (S-F coupling) at the regional level, which was then correlated with age to explore its physiological effects. Structural connectivity (SC) based on CTh and functional connectivity (FC) based on glucose metabolism were constructed followed by exploring the network similarity and coupling between SC and FC. The global and local efficiency of the brain SC and FC were also evaluated.

Results: 97.83% of subjects exhibited a significant negative correlation between regional CTh and FDG uptakes ($p<0.05$ with FDR correction), and this S-F coupling was negatively correlated with age ($r=-0.35$, $p<0.001$). At the connective level, SC-FC coupling was almost positive, with more regions in the old age group exhibiting significant coupling than in the middle age group. Besides, FC exhibited denser connections than SC, resulting in both higher global and local efficiency, but lower global efficiency when the network size corrected.

Conclusion: This study found there is a coupling between CTh and glucose metabolism from the regional to connective level. These findings may have implications for the diagnosis and treatment of

 doi.org/10.32388/DUOS00

neurological and psychiatric disorders.

Clinical relevance statement: The observed coupling between brain cortical thickness and glucose metabolism, both at the regional and connective level provides insights into the brain mechanisms and highlights potential implications for the diagnosis and treatment of neurological and psychiatric disorders.

Qi Huang, Yihong Yang, and Na Qi contributed equally to this work.

Corresponding authors: Fengchun Hua, huafc@hotmail.com; Shuhua Ren, karen96_ren@126.com; Fang Xie, fangxie@fudan.eu.cn

Abbreviations

CTh, cortical thickness; E_{glob}, global efficiency; E_{loc}, local efficiency; FC, functional connectivity; SC, Structural connectivity; S-F coupling, structural and functional coupling; K, average network degree

Key points

1. Human brain structure and function were coupled to complete complex tasks.
2. Brain cortical thickness and glucose metabolism were negatively coupled at the regional level but positively correlated at the connective level.
3. Brain structural and functional coupling reflects aging progress, and can be applied in the diagnosis of brain disorders.

Keywords: Brain, PET/MRI, cortical thickness, glucose metabolism, structural and functional coupling.

Introduction

The human brain is an intricately organized system, where the structure and function of different regions work together to accomplish complex tasks. Disruption of the delicate balance between brain structure and function has been proven to be implicated in several neurological and psychiatric disorders [1][2][3][4]. Therefore, understanding the relationship between brain structure and function is a critical question in human neuroscience.

Cortical thickness (CTh) and glucose metabolism are two widely used measures in brain research. CTh, measured by MRI, refers to the distance between two borders of the gray matter; and glucose metabolism, measured by ^{18}F-FDG PET, reflects neuronal activity. These two measures provide opportunities to investigate the brain structures and functions, and trajectories of CTh and glucose metabolism might not change synchronously during aging or in disease states, as it is reported that aging was negatively correlated with CTh in many cortical regions but with decreased mean brain glucose metabolism only in the temporal lobe [5]. Thus, we would expect that the coupling of the two modalities would provide unique and distant sources of variability.

Large-scale brain networks have emerged as a promising tool to study the brain. In brain network models, nodes correspond to brain regions, whereas edges correspond to connections between the nodes. Structural connectivity (SC) constructed based on brain CTh, defines anatomical connections between two regions showing statistically significant correlations in CTh. Previous studies validated that CTh-based SC provides crucial connectivity information in the human brain [6][7], and is consistent with known neuroanatomical pathways measured by diffusion imaging [8]. Functional connectivity (FC) constructed using ^{18}F-FDG PET images, assumes that brain regions with similar metabolic demands are also functionally connected [9][10]. Compared to the most widely used FC constructed by the BOLD-fMRI, metabolic FC constructed in an inter-subject way could convey similar neural networks, and provide complementary insight into the neuromechanism [11]. Previous studies showed that most functional links were not supported by an underlying structural link, and functional communities tend to encompass spatially distributed systems with perceptual, cognitive, and affective relevance, while structural networks tend to be more spatially constrained [12]. Such observations highlight the need to consider multimodal brain connectomes simultaneously to understand disease pathophysiology.

In the present study, we aimed to investigate the coupling between human brain CTh and glucose metabolism using ^{18}F-FDG PET/MRI. We (1) explored the regional relationship between CTh and glucose metabolism across the cortex and whether this relationship reflected aging progress; (2) constructed the structural and functional brain network, and explored the similarity and SC-FC coupling between the structural and functional brain network in group-level; and (3) compared the topological properties of structural and functional brain networks.

Materials and Methods

Subjects

Two hundred and one subjects who performed whole-body ^{18}F-FDG PET/MR between August 2020 and September 2021 in the Department of Nuclear Medicine, Shanghai East Hospital were retrospectively enrolled. All subjects were clinically evaluated, and their whole-body PET/MRI images were reviewed by two nuclear medicine physicians (N.Q., and J.Z). Subjects who had a stroke, major head trauma, neuropsychiatry disorders, malignancy, uncontrolled diabetes, medicine abuse, or alcohol addiction were excluded. Finally, 138 subjects were included and divided into two groups based on their age: middle age and old age group.

PET/MR Scanning

All subjects underwent whole-body ^{18}F-FDG PET/MR scanning using a uPMR 790 HD TOF PET/MR system (United Imaging Healthcare, Shanghai, China). The subjects fasted for at least 6 hours to keep their blood glucose level <6.0 mmol/L before injection. They were intravenously injected with a dose of ~5.5 MBq/kg of ^{18}F-FDG and rested quietly for about 60 min. Then a 10-min brain PET was acquired simultaneously with an MRI T1 image after the whole-body PET/MR scanning. The brain MRI T1 images were acquired with the following parameters: echo time = 3 ms, repetition time = 7.19 ms, inverse time = 750 ms, flip angle = 10°, slice thickness = 0.67 mm, spacing between slices = 0.67 mm, data matrix = 264×460×512 mm, and voxel size = 0.67×0.5×0.5 mm. Brain PET images were reconstructed using the OSEM algorithm, with 3 iterations and 20 subsets followed by a Gaussian filter of 4 mm in full width at half maximum on a 150×150×159 mm matrix with a 2×2×2 mm voxel size, and corrected for decay, normalization, photon attenuation, scatter, and random coincidences.

Image Preprocessing

The T1 images were preprocessed using the computational anatomy toolbox (CAT12, http://www.neuro.uni-jena.de/cat/) and SPM12 (http://www.fil.ion.ucl.ac.uk/spm) with the default settings, including skull-stripping, denoising, correction for bias field inhomogeneities. Then the images were segmented into gray matter, white matter, and cerebrospinal fluid, and normalized using the Shooting registration algorithm. Volumes were segmented using surface and thickness estimation based on projection-based thickness and export of ROI data using the Desikan-Killiany atlas [13] in the writing

options. In addition to CTh, the local gyrification index, sulcus depth, fractal dimension as well as regional cortical volume were also extracted using standard procedures for ROI extraction provided in CAT12.

The PET images were preprocessed using SPM12. All images were co-registered to their corresponding T1 image and spatially normalized into Montreal Neurological Institute space using the transformation parameters estimated on the corresponding T1 image. Then the Desikan-Killiany atlas [13] was applied to segment the cerebral cortex into 68 regions (34 for each hemisphere without cerebellum), and the mean intensity of each region was extracted. In addition, the regional FDG uptake values were also corrected to partial volume affected using the Geometric Transfer Matrix correction algorithm [14] to exclude the effect of brain atrophy.

Network Construction

Prior to the brain network construction, linear regression was performed on regional CTh or FDG values to remove the mean CTh or FDG uptakes of the whole brain, and the residuals substituted for the raw CTh or FDG values. SC and FC were constructed by calculating Spearman's rank correlation coefficients between the residual CTh or FDG values of each pair of brain regions in an inter-subject manner, and the spurious connections were excluded with a coefficient threshold of $p>0.05$. In the network, the node was defined as a brain region, and the edge was defined as a connection of each pair of nodes with the weight of the edge defined as the absolute value of correlation coefficients.

Based on the above constructed structural and functional network, we first explored the similarity between SC and FC by calculating the probability of the existence of FC while structurally connected, i.e., P(existence|connected), and the probability of inexistence of FC while structural disconnected, i.e., P(inexistence|disconnected). The higher values of P(existence|connected) and P(inexistence|disconnected) indicated a higher similarity between the two networks. To explore the age effect on the brain connectome, we also calculated the P(existence|connected) and P(inexistence|disconnected) of structural or functional connectivity between the middle and old age groups, with the middle age group as the denominator.

Network properties

The network size is reflected by the average network degree (K), which is calculated as $K = \frac{1}{N}\sum_I k_i$, where k_i is the sum of the weights attached to node *i*, and *N* is the number of nodes. The mean network

degree is commonly used as a measure of density, or the total “wiring cost” of the network.

We then calculated the global and local efficiency of the above-constructed network. Global efficiency is a measure of network integration, which is inversely related to path length defined as $E_{glob} = \frac{1}{N(N-1)} \sum_{i \neq j} \frac{1}{d_{ij}}$, where d_{ij} is the shortest weight path length between node *i* and *j*. The local efficiency (E_{loc}) is a measure of network segregation, and is defined as the average nodal efficiency: $E_{loc} = \frac{1}{N} \sum_{i \in G} E(G_i)$, where G_i is the subgraph of the neighbors of *i*. Both global and local efficiency express the very precise physical meaning of the efficiency of transporting information, including local necessities (fault tolerance) and wide-scope interactions[15].

To exclude the effect of network size on the global and local efficiency, the networks were binarized using a set of connective densities from 0.01 to 0.17 with a step of 0.02, and the network efficiencies were calculated on the binarized network at each density.

Statistics

As the data were non-normal distributed, Spearman’s rank correlation coefficient was calculated between the CTh and FDG values of the series of 68 regions for each subject to explore the structural and functional coupling (S-F coupling) at the regional level. Then the association between S-F coupling and age was calculated to explore its physiological effects. To explore the coupling between brain structural and functional connectivity (SC-FC coupling), the correlations between the SC and FC matrix were calculated for the two groups respectively., as shown in Fig. 1b.

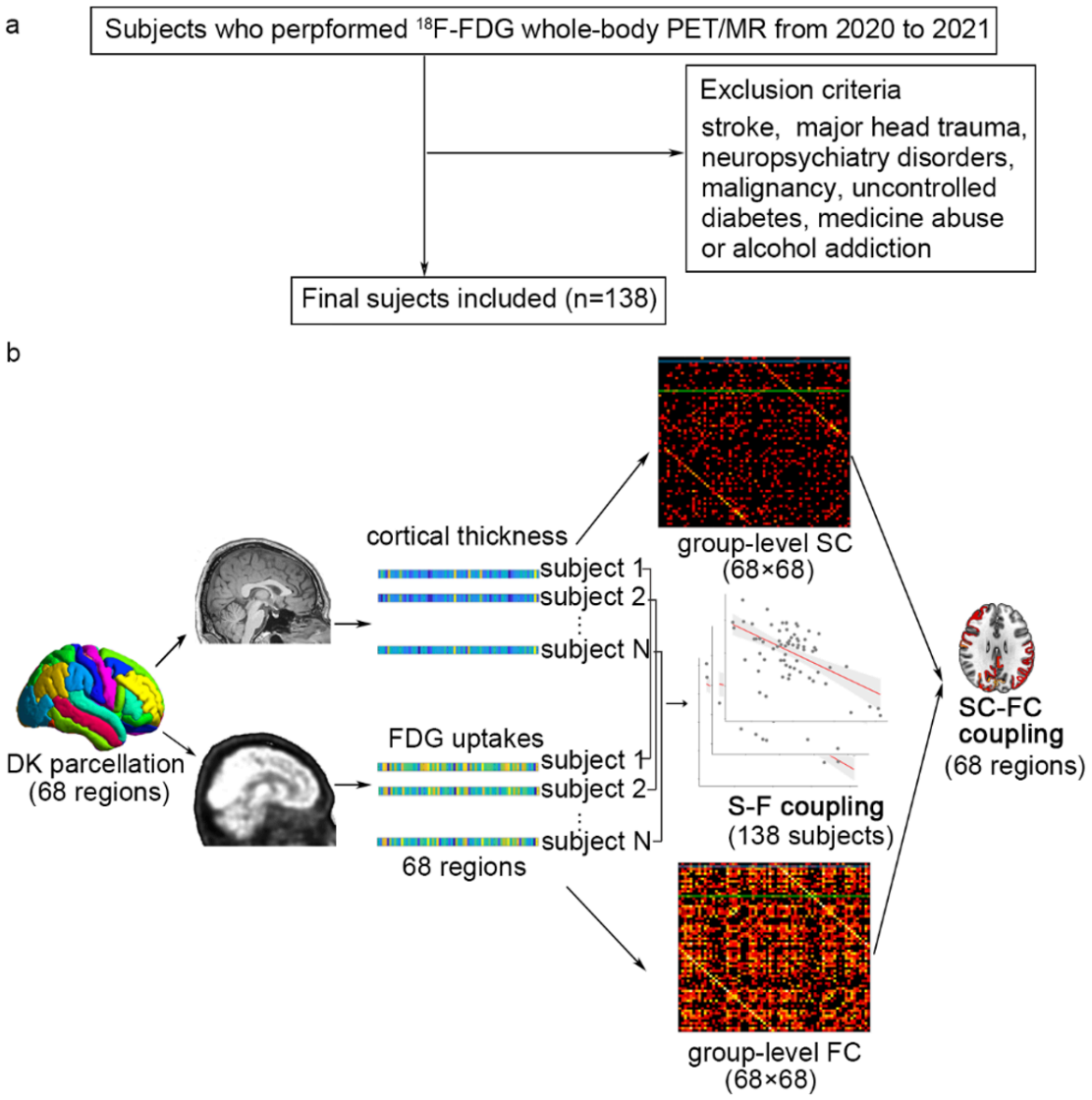

Fig. 1. Flowchart for (a) subjects' enrollment and statistics.

Results

Demographics

Gender distribution between the two groups was not significantly different, and detailed information was provided in Table 1.

	Middle age group	Old age group
Sample size	69	69
Gender (male/female)	41/28	41/28
Age (years, mean±SD)	42.33±5.25	60.19±4.88
Age range (years)	21-49	55-73

Table 1. Demographics

S-F Coupling

The brain S-F were negatively coupled at the regional level. In detail, 135 out of 138 (97.83%) subjects exhibited a significant negative correlation between CTh and FDG ($p<0.05$ with FDR correction), and the Spearman's rank coefficients ranged from -0.11 to -0.71, as shown in Fig. 2. We further discovered that this S-F coupling was negatively correlated with age (R=-0.35, p<0.001), which were also confirmed when the FDG images were partial volume corrected (R=-0.27, p=0.0017, sFig 1), those results suggested that discordancy between brain structure and function was larger during aging.

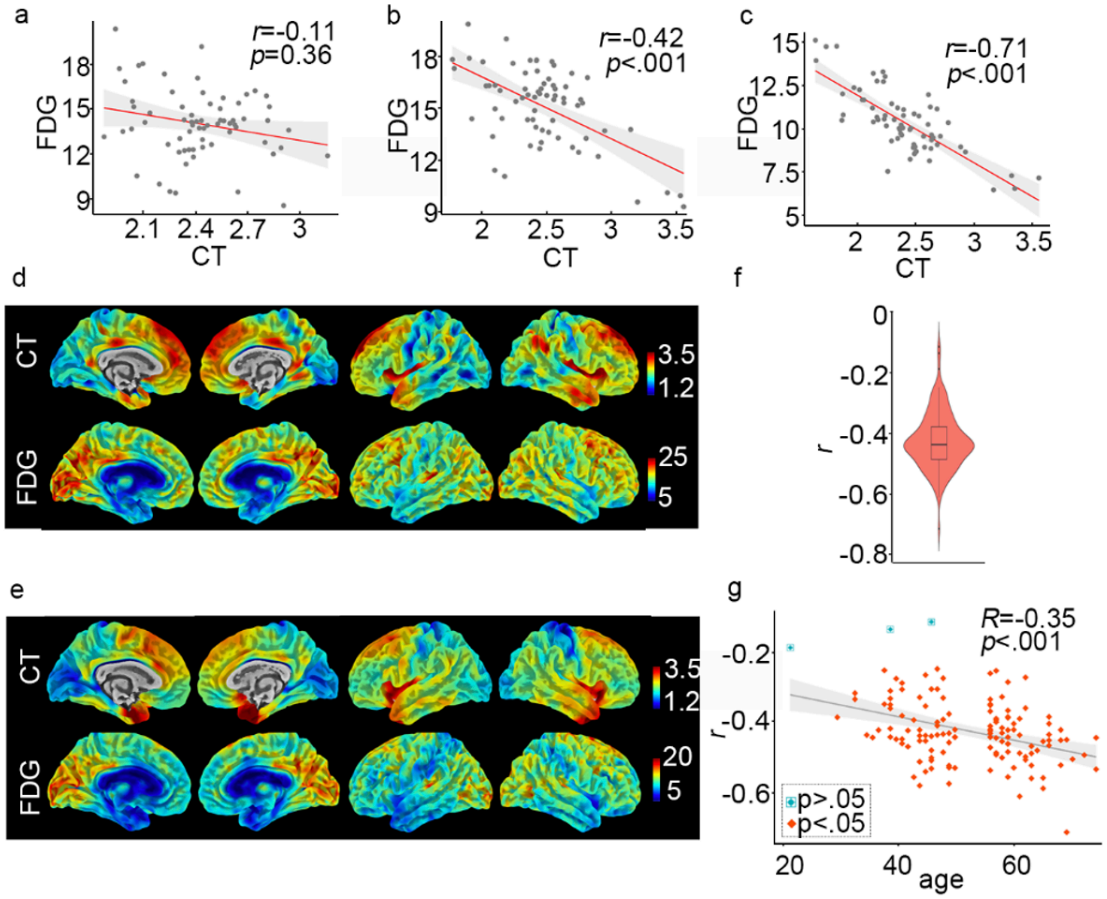

Fig. 2. Regional S-F coupling. Scatters of regional FDG and CT values, as well as the images of subjects with minimum (A, D) and maximum (C, E) coupling discordance; correlative scatter of subject with the median S-F coupling was also provided (B). (F) is the total S-F coupling strength distribution, and S-F coupling was negatively associated with age (G). the y-axis of (A)-(C) were the PET values $*10^3$.

Network Similarity

The FC and SC matrix for the middle and old age groups were shown in Fig. 3. We first investigated the network similarity based on the hypothesis that SC is the basis and the constraint for the FC. We found that the old age group exhibited more similarity between SC and FC especially when SC is connected and FC exists. In detail, P(existence|connected) =0.5431 and 0.6876, and P(inexistence|disconnected) =0.4995 and 0.5260 for the middle and old age population. Permutation tests showed that P(existence|connected) between the young and old population was statistically significant ($p<0.001$), while P(inexistence|disconnected) was not ($p=0.3426$).

doi.org/10.32388/DUOS00

During aging, FC exhibited higher P (existence|connected) (0.7986 and 0.3858 for the FC and SC; $p<0.001$, FDR corrected), and lower P(inexistence|disconnected) (0.7105 and 0.8461 for FC and SC; $p=0.0045$, FDR corrected), which means that connections across life-span were sustained in FC, and disconnections across life-span were sustained in SC.

SC-FC Coupling

Based on the brain's functional and structural networks, we explored the SC-FC coupling. Unlike the individual negative S-F coupling, the SC-FC couplings were almost positive and varied across the cortex, ranging from -0.12 to 0.42 for the middle age group, and -0.19 to 0.58 for the old age group. In the middle age group, only three regions, including the left cuneus, left lingual, and right paracentral region showed significant SC-FC coupling (Fig. 3c). While in the old age group, 27 out of 68 regions showed significant SC-FC coupling ($p<0.05$, FDR corrected). Regions exhibited significant SC-FC coupling almost evenly distributed across the brain, in detail, 7 regions in the frontal lobe, including bilateral frontal pole, paracentral gyrus, right precentral region, right rostral middle frontal gyrus, left orbital and triangular part of inferior frontal gyrus; 6 in the occipital lobe, including bilateral cuneus, pericalcarine, right lingual and lateral occipital gyrus; 7 in parietal, including bilateral postcentral gyrus, left inferior parietal gyrus, supramarginal gyrus, isthmus cingulate cortex, right precuneus and superior parietal gyrus; 5 in temporal lobe, including bilateral fusiform, left inferior temporal gyrus, right middle temporal gyrus and parahippocampal gyrus; as well as right insula, as shown in Fig. 3f. Besides, three regions including right frontal pole, right insula and right postcentral regions showed significant higher SC-FC coupling in old age than the middle age group.

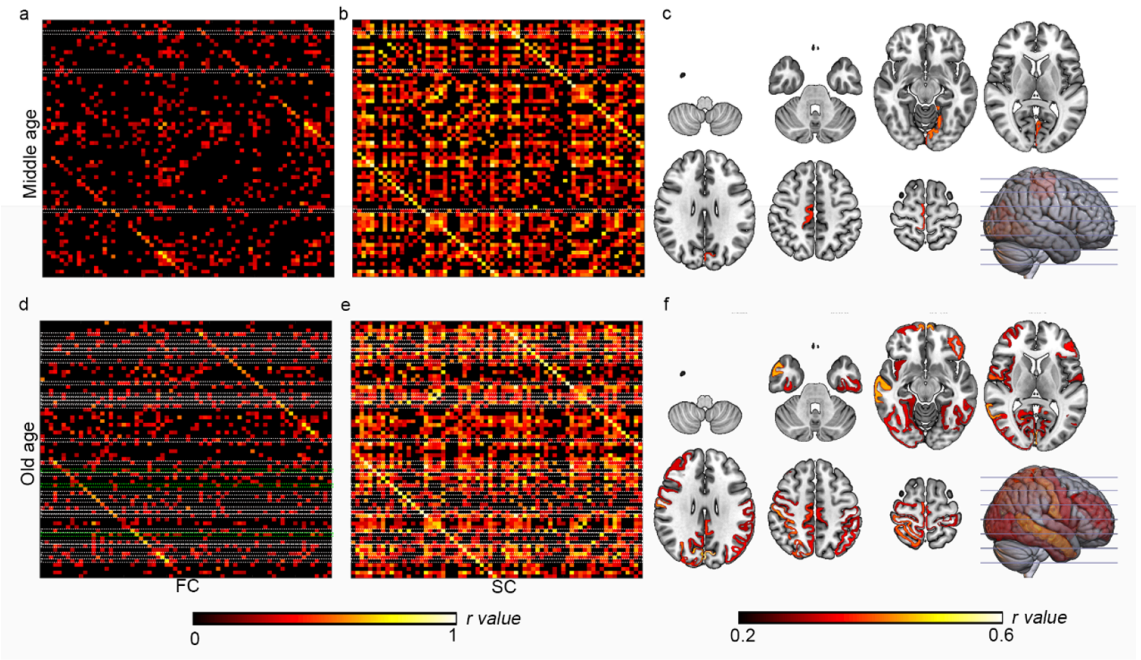

Fig. 3 The brain structural (A, D) and functional (B, E) network for the middle and old age group. The dotted rectangular indicated the significantly correlated connections between FC and SC, and the green dotted rectangular regions showed significantly stronger connections in the old than middle age group. The positions of those regions were shown in C and F.

<

The network properties including degree, global and local efficiency were calculated to explore the segregation and integration of the brain networks (Fig. 4). FC (K =14.1037, 15.5055 for middle and old age groups, respectively) exhibited significantly denser connections compared to SC (K = 3.7373, 4.3927 for middle and old age group, respectively) in both middle and old age group ($p<0.001$). Thus, it was reasonable to get the result that FC ($E_{glob} = 0.33, 0.34 \quad E_{loc} = 0.38, 0.39$ for the middle and old age group) had higher global and local efficiency the SC ($E_{glob} = 0.18, 0.19 \quad E_{loc} = 0.18, 0.22$ for the middle and old age group). But when the network size was corrected, the local efficiency was significantly higher in FC than that in SC in both the middle and old age groups, while the global efficiency was the opposite, as shown in Fig 4.

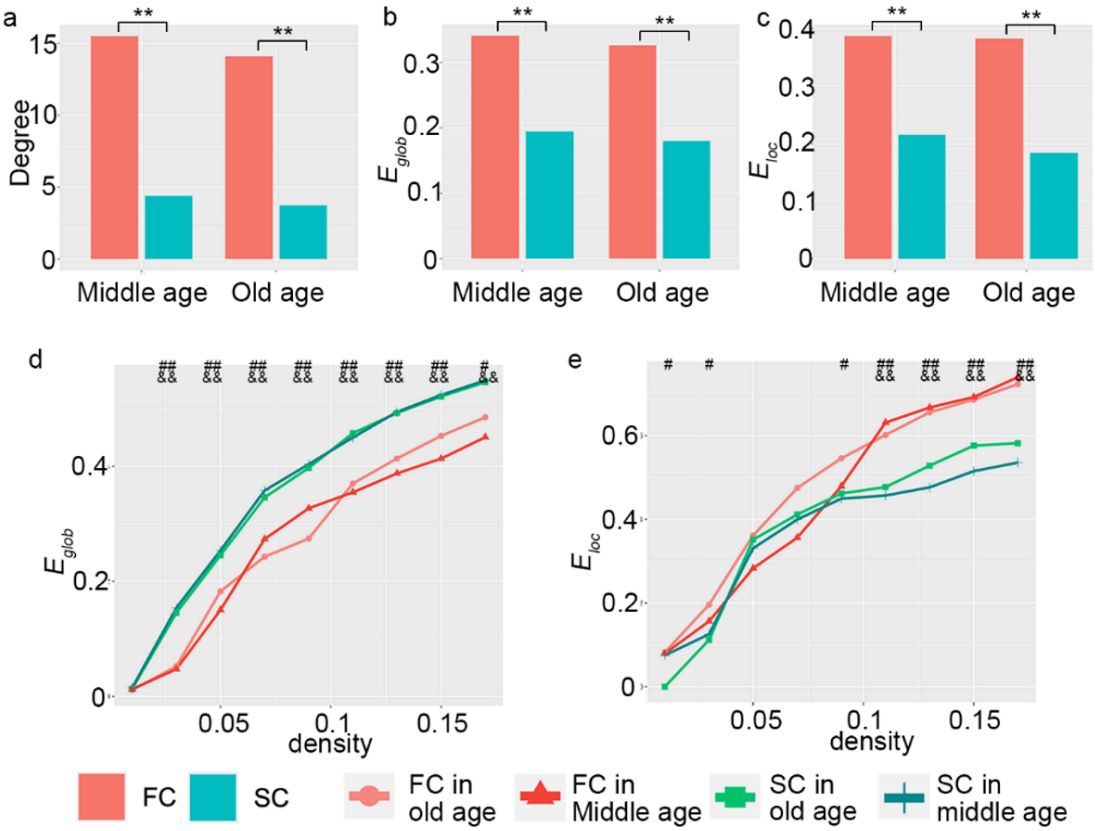

Fig. 4. Network properties of the SC and FC in middle and old age groups. network degree (A), global efficiency(B) and local efficiency(C) of the brain network. Global efficiency (D) and local efficiency (E) were also calculated on the binarized networks to exclude the effect of network size. **, permutation test p<0.001 with FDR correction between middle and old age group; $^{\#}$ p<0.05 with FDR correction for the FC and SC difference in old age group; $^{\#\#}$ p<0.001 with FDR correction for the FC and SC difference in old age group; $^{\&}$ p<0.05 with FDR correction for the FC and SC difference in middle age group; $^{\&\&}$ p<0.001 with FDR correction for the FC and SC difference in middle age group.

Discussion

In this study, we quantified the coupling between brain structure and function at regional and connective levels. Our findings demonstrated that CTh and FDG uptakes were negatively correlated at the regional level and this discordancy was larger during aging. At the connective level, SC-FC was positively coupled, and the old age group exhibited more similarities between SC and FC. Besides, the connections were denser in the FC matrix, partly resulting in higher global and local network efficiency in FC than SC, but

FC exhibited lower global efficiency and higher local efficiency than SC when the network size is corrected.

Surface-based morphometry offers more information about brain structure. Except for CTh, cortical characteristics include sulcal depth, gyrification index, and fractal dimension. The sulcal depth and gyrification index are shape-based quantification to provide information about cortical folding[16]. The fractal dimension was used to describe the geometrical properties of structural complexity in the cerebral cortex [17]. We found sulcal depth and fractal dimension did not show any significant correlation with regional glucose metabolism, while the gyrification index showed a significant correlation with regional glucose metabolism, but this correlation could not reflect the aging progress (sFig 1). Taken together, surface parameters reflecting shape complexity had no correlation with glucose metabolism or the correlation could not reflect aging progress, so CTh was chosen as a representation of brain structure.

CTh reflects the size, density, and arrangement of cells, allowing for in vivo acquisition of valuable information about neuroanatomy. Similar to the previous study that CTh is not correlated with the total intracranial volume [18], our results confirm that CTh is independent of the regional volume (sFig 1), but is negatively correlated with FDG uptake for a subject, with a stronger discordance during aging. Previous studies confirmed that metabolic costs of the brain were in proportion to the total surface area of the neuronal membrane [19], and CTh and surface area constitute the cortical gray volume, but change independently from each other [20]. As age affects CTh and brain glucose metabolism in different ways[5], the negative association between CTh and glucose metabolism may reflect a shift in the balance between energy consumption and neurodegeneration.

At the connective level, we found a positive association between SC and FC, with more regions exhibiting significant correlations during aging. This result is consistent with the observation that the old age group exhibited higher P(existence|connected) than the middle age group. The function is constrained by the underlying structure, but there is no one-to-one mapping, large-scale dynamic functional coordination exists within a fixed structural architecture[21], which means that the brain was elastic and plastic. Functional interactions may arise via indirect structural connections, resulting in the functional connection among regions that are two or more synapses removed from each other. In other words, the functional connection of two regions is driven not only by direct signaling between them, but also by common inputs they receive from sensory organs and from the entire network [12]. Previous studies reported that a stronger coupling of SC and FC is related to poorer cognitive performance and decreasing

awareness/consciousness [22][23][24]. Here, we also found the SC-FC coupling was extended from basic sensorimotor to high-level functions during aging.

In the present study, we found that FC exhibited a higher degree than SC, which was similar to previous studies using diffusion tensor imaging and resting-state fMRI [25][26]. The functional network is based on patterns of synchronized neural activity between different brain regions, rather than on the presence or absence of anatomical connections between these regions, that is, FC can include indirect or polysynaptic connections, which may not be captured by the structural connectivity. As a result, functional networks can have more connections than structural networks. Besides, the functional network can exhibit a high degree of redundancy, with multiple connections between the same pair of brain regions. This redundancy can provide robustness and resilience to the network, allowing it to continue functioning even if some connections are disrupted or lost. In contrast, the structural network tends to have fewer connections, with a greater emphasis on efficiency and minimizing wiring costs. The higher degree of FC consequently induced the higher global and local efficiency of FC than SC. While FC have been found to exhibit lower integration and higher segregation than SC when corrected for the network size, which may seem counterintuitive given that FC is thought to be shaped by the underlying SC of the brain. One possible explanation is that FC are shaped not only by the underlying SC, but also by ongoing neural activity and the dynamic patterns of information flow that emerge from this activity. The dynamic nature of functional connectivity means that the network may exhibit more transient and flexible segregation patterns that are adapted to the task at hand, rather than a fixed modular organization that is determined by the underlying anatomy. This could lead to lower integration and higher segregation in FC compared to SC.

However, there are several limitations of the present study. Firstly, subjects aged from 21 to 73 years old were involved in this study. The age range was too broad to capture the precise aging process, and did not include individuals in the developmental process. Besides, previous studies demonstrated that brain structure and function are modulated by gender, race, and cultural background, the effects of those factors on the coupling of brain structure and function are interesting fields to be studied in the future.

In conclusion, we quantified the coupling between the brain structure and function from regional to connective level using ^{18}F-FDG PET/MRI. We demonstrated that the CTh and FDG uptakes were negatively coupled, and this discordancy was larger during aging. At the connective level, SC-FC is positively coupled and the regions exhibiting SC-FC coupling covered from primary to high-level

functions. Those findings provide a comprehensive picture of the coupling between brain structure and function and would provide a unique source of variations underlying brain aging and disease.

Acknowledgements

We thank the staff of the Department of Nuclear Medicine, Shanghai East Hospital, Tongji University School of Medicine for data acquisition.

Funding

This study has received funding from the National Key R&D Program of China (2022YFC3603003); the National Natural Science Foundation of China [82201583, 8217052097, 82071962]; Shanghai Municipal Health Commission fund (202040420), Shanghai Municipal Key Clinical Specialty [shslczdzk03402], Shanghai Municipal Science and Technology Major Project [2018SHZDZX01] and ZJLab; STI2030-Major Projects (022ZD0213800), Key Discipline Construction Project of Shanghai Pudong New Area Health Commission (PWZxk2022-12).

Other References

- Tamnes, C.K., Ostby, Y., Fjell, A.M., Westlye, L.T., Due-Tonnessen, P., Walhovd, K.B. (2010). Brain maturation in adolescence and young adulthood: regional age-related changes in cortical thickness and white matter volume and microstructure. Cerebral Cortex, 20, 534-548.
- Palejwala, A.H., Dadario, N.B., Young, I.M., et al. (2021). Anatomy and White Matter Connections of the Lingual Gyrus and Cuneus. World Neurosurgery, 151, e426-e437.
- Aminoff, E.M., Kveraga, K., Bar, M. (2013). The role of the parahippocampal cortex in cognition. Trends in Cognitive Sciences, 17, 379-390.
- Cavanna, A.E., Trimble, M.R. (2006). The precuneus: A review of its functional anatomy and behavioural correlates. Brain, 129, 564-583.
- Alahmadi, A.A.S. (2021). Investigating the sub-regions of the superior parietal cortex using functional magnetic resonance imaging connectivity. Insights into Imaging, 12, 47.
- Onitsuka, T., Shenton, M.E., Salisbury, D.F., et al. (2004). Middle and inferior temporal gyrus gray matter volume abnormalities in chronic schizophrenia: an MRI study. The American Journal of Psychiatry, 161, 1603-1611.

- Belyk, M., Brown, S., Lim, J., Kotz, S.A. (2017). Convergence of semantics and emotional expression within the IFG pars orbitalis. NeuroImage, 156, 240-248.
- Foundas, A.L., Leonard, C.M., Gilmore, R.L., Fennell, E.B., Heilman, K.M. (1996). Pars triangularis asymmetry and language dominance. Proceedings of the National Academy of Sciences, 93, 719-722.
- Weiner, K.S., Zilles, K. (2016). The anatomical and functional specialization of the fusiform gyrus. Neuropsychologia, 83, 48-62.
- Huang, Q., Ren, S., Zhang, T., et al. (2021). Aging-related modular architectural reorganization of the metabolic brain network. Brain Connectivity, 10.1089/brain.2021.0054.

References

1. ^ *Wang, J., Khosrowabadi, R., Ng, K. K., et al. (2018). Alterations in brain network topology and structural-functional connectome coupling relate to cognitive impairment. Frontiers in Aging Neuroscience, 10.*
2. ^ *Cao, R., Wang, X., Gao, Y., et al. (2020). Abnormal anatomical rich-club organization and structural-functional coupling in mild cognitive impairment and Alzheimer's disease. Frontiers in Neurology, 11.*
3. ^ *Kuceyeski, A., Shah, S., Dyke, J. P., et al. (2016) The application of a mathematical model linking structural and functional connectomes in severe brain injury. NeuroImage: Clinical, 11, 635-647.*
4. ^ *Zhang, R., Shao, R., Xu, G., et al. (2019). Aberrant brain structural-functional connectivity coupling in euthymic bipolar disorder. Human Brain Mapping, 40, 3452-3463.*
5. a, b *Baik, K., Jeon, S., Yang, S.-J., et al. (2023). Cortical thickness and brain glucose metabolism in healthy aging. Journal of Clinical Neurology, 19, 138-146.*
6. ^ *He, Y., Chen, Z., Evans, A. (2008). Structural insights into aberrant topological patterns of large-scale cortical networks in Alzheimer's disease. Journal of Neuroscience, 28, 4756-4766.*
7. ^ *Qi, T., Gu, B., Ding, G., et al. (2016). More bilateral, more anterior: Alterations of brain organization in the large-scale structural network in Chinese dyslexia. Neuroimage, 124(Part A), 63-74.*
8. ^ *He, Y., Chen, Z.J., Evans, A.C. (2007). Small-world anatomical networks in the human brain revealed by cortical thickness from MRI. Cerebral Cortex, 17, 2407-2419.*
9. ^ *Horwitz, B., Duara, R., Rapoport, S.I. (1984). Intercorrelations of glucose metabolic rates between brain regions: Application to healthy males in a state of reduced sensory input. Journal of Cerebral Blood Flow & Metabolism: Official Journal of the International Society of Cerebral Blood Flow & Metabolism, 4, 484.*

10. ^Macko, K.A., Jarvis, C.D., Kennedy, C., et al. (1982). Mapping the primate visual system with [2-14C] deoxyglucose. Science, 218, 394-397.

11. ^Di, X., Gohel, S., Thielcke, A., Wehrl, H.F., Biswal, B.B., Alzheimer's Disease Neuroimaging I (2017). Do all roads lead to Rome? A comparison of brain networks derived from inter-subject volumetric and metabolic covariance and moment-to-moment hemodynamic correlations in old individuals. Brain Structure & Function, 222, 3833-3845.

12. a, bSuarez, L.E., Markello, R.D., Betzel, R.F., Misic, B. (2020). Linking structure and function in macroscale brain networks. Trends in Cognitive Sciences, 24, 302-315.

13. a, bDesikan, R.S., Ségonne, F., Fischl, B., et al. (2006). An automated labeling system for subdividing the human cerebral cortex on MRI scans into gyral-based regions of interest. NeuroImage, 31, 968-980.

14. ^Gonzalez-Escamilla, G., Lange, C., Teipel, S., Buchert, R., Grothe, M.J., Alzheimer's Disease Neuroimaging Initiative (2017). PETPVE12: an SPM toolbox for Partial Volume Effects correction in brain PET: Application to amyloid imaging with AV45-PET. NeuroImage, 147, 669-677.

15. ^Latora, V., Marchiori, M. (2001). Efficient behavior of small-world networks. Physical Review Letters, 87, 198701.

16. ^Lyu, I., Kang, H., Woodward, N.D., Landman, B.A. (2018). Sulcal depth-based cortical shape analysis in normal healthy control and schizophrenia groups. Proceedings of SPIE - The International Society for Optical Engineering, 10574.

17. ^Im, K., Lee, J.M., Yoon, U., et al. (2006). Fractal dimension in human cortical surface: multiple regression analysis with cortical thickness, sulcal depth, and folding area. Human Brain Mapping, 27, 994-1003.

18. ^Barnes, J., Ridgway, G.R., Bartlett, J., et al. (2010). Head size, age, and gender adjustment in MRI studies: a necessary nuisance? NeuroImage, 53, 1244-1255.

19. ^Bullmore, E., Sporns, O. (2012). The economy of brain network organization. Nature Reviews Neuroscience, 13, 336.

20. ^Frye, R.E., Liederman, J., Malmberg, B., McLean, J., Strickland, D., Beauchamp, M.S. (2010). Surface area accounts for the relation of gray matter volume to reading-related skills and history of dyslexia. Cerebral Cortex, 20, 2625-2635.

21. ^Shen, K., Hutchison, R.M., Bezgin, G., Everling, S., McIntosh, A.R. (2015). Network structure shapes spontaneous functional connectivity dynamics. The Journal of Neuroscience, 35, 5579-5588.

22. ^Barttfeld, P., Uhrig, L., Sitt, J.D., Sigman, M., Jarraya, B., Dehaene, S. (2015). Signature of consciousness in the dynamics of resting-state brain activity. Proceedings of the National Academy of Sciences of the United Stat

es of America, 112, 887-892.

23. ^*Wang, J., Khosrowabadi, R., Ng, K.K., et al. (2018). Alterations in Brain Network Topology and Structural-Functional Connectome Coupling Relate to Cognitive Impairment. Frontiers in Aging Neuroscience, 10, 404.*
24. ^*Gu, Z., Jamison, K.W., Sabuncu, M.R., Kuceyeski, A. (2021). Heritability and interindividual variability of regional structure-function coupling. Nature Communications, 12.*
25. ^*Chen, Q., Lv, H., Wang, Z., et al. (2022). Distinct brain structural-functional network topological coupling explains different outcomes in tinnitus patients treated with sound therapy. Human Brain Mapping. doi: 10.1002/hbm.25848*
26. ^*Sporns, O. (2013). Structure and function of complex brain networks. Dialogues in Clinical Neuroscience, 15, 247-262.*

Supplementary data: available at https://doi.org/10.32388/DUOS00

Declarations

Funding: This study has received funding from the National Key R&D Program of China (2022YFC3603003); the National Natural Science Foundation of China {m/82201583,8217052097,82071962/}; Shanghai Municipal Health Commission fund (202040420), Shanghai Municipal Key Clinical Specialty [shslczdzk03402], Shanghai Municipal Science and Technology Major Project [2018SHZDZX01] and ZJLab; STI2030-Major Projects (022ZD0213800), Key Discipline Construction Project of Shanghai Pudong New Area Health Commission (PWZxk2022-12).

Potential competing interests: No potential competing interests to declare.